Radiocarbon, Vol 61, Nr 4, 2019, p 1077–1089 DOI:10.1017/RDC.2019.43

OPTIMIZED VOLUME DETERMINATIONS AND UNCERTAINTIES FOR ACCURATE AND PRECISE MANOMETRY

Xi Lu* • Steven R Beaupré

School of Marine and Atmospheric Sciences, Stony Brook University, Stony Brook, NY 11794-5000 USA

ABSTRACT. Precise manometric pressure, volume, and temperature (P-V-T) measurements of carbon in samples, standards, and blanks are critical for radiocarbon studies. While P and T uncertainties depend on instrument choice and environmental stability, V uncertainties depend on their method of measurement and are often overlooked. We used numerical simulations and error propagation to find optimum procedures for measuring "cold-finger" volumes equipped with capacitance diaphragm gauges (CDGs) by two common application of Boyle's Law: cryogenic transfers and serial gas expansions with a reference flask of known volume. Minimum relative uncertainties of cold-finger volumes are comparable for these two methods (~0.002), but the serial gas expansion method is preferred due to its convenience. Serial gas expansions can be performed to high precision by using dry air, an initial pressure ~76% full-scale (e.g., 760 Torr), and a reference flask with an optimal volume based on preliminary estimates of cold-finger volumes and an empirical power function. The volumes of cold-fingers $\geq$ 12 cm^3 can be determined with minimum achievable relative uncertainties of 0.0021 to 0.0023. This limit translates to minimum achievable relative uncertainties of 0.0026 to 0.0027 for P-V-T measurements of moles of gas simulated here.

KEYWORDS: capacitance diaphragm gauges, manometry, optimization, uncertainty, vacuum line.

INTRODUCTION

Measurements of the mass of carbon in samples, standards, and blanks are used for radiocarbon (^{14}C) blank corrections, sample preparation, quality control, age determinations, source apportionment calculations, geochemical interpretations, and splitting of aliquots for complementary measurements (e.g., $\delta^{13}C$) (e.g., Reimer et al. 2004, 2009, 2013; Beaupré et al. 2007, 2016; Shah Walter et al. 2015). These masses are commonly and conveniently determined manometrically because nearly all samples, standards, and blanks are converted to CO_2 gas prior to graphitization and/or ^{14}C measurements. This is accomplished by applying an appropriate equation of state to determine the number of moles (n) of C from measurements of temperature (T) and the pressure (P) exerted by CO_2 in a container of known volume (V; a "cold-finger," "measuring volume," "calibrated volume," etc.). Consequently, manometric measurement uncertainties depend on the magnitudes and uncertainties of P, T, V, and additional parameters from the equation of state (e.g., virial coefficients). Whereas the accuracy and precision of P and T are largely limited by instrumentation and the uniformity of ambient conditions (e.g., T, humidity) (Hyland and Shaffer 1991), the accuracy and precision of cold-finger volume measurements can be improved through experimental design. Previous reports (e.g., Rees and Ross 1964) recognized the importance of system design, such as flask pairing, in minimizing the variance of gas quantity measurements and subsequent calculations. However, most of these works took the variance in manometer flask size as a constant, thus ignoring the influence of system design and determination procedures on the relative uncertainty of cold-finger volume measurements. Therefore, optimizing the procedure for measuring cold-finger volumes is potentially a practical, low-cost approach to improve the precision of manometric measurements and the ability to answer scientific questions.

Frequently, manometric systems use capacitance diaphragm pressure gauges (CDG's) because they are relatively affordably high-precision pressure sensors (Hamme and Emerson 2004; Beaupré et al. 2007, 2016; Leigh McCallister and del Giorgio 2008; Shah Walter et al. 2015; Gospodinova et al. 2016). However, cold-finger volumes cannot be determined gravimetrically with liquids of known density because the attached CDG's are sensitive electronic instruments

*Corresponding author. Email: xi.lu@stonybrook.edu.

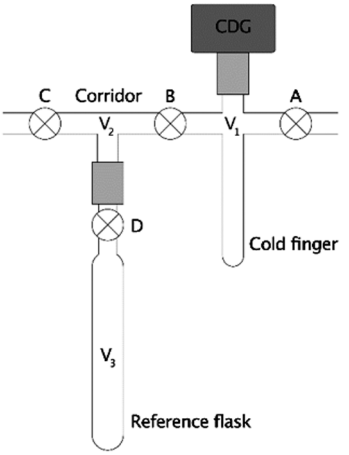

Figure 1 Section of a typical vacuum line assembly. The system consists of a cold-finger (V_1), corridor (V_2), reference flask of known volume (V_3), valves (⊗; labeled A, B, C, and D), a pressure gauge (dark gray rectangle), and Ultra-Torr vacuum fittings (light gray rectangles) to connect some components.

held in a fixed position on the vacuum line (Figure 1). Instead, two common procedures for measuring this volume (V_1) include cryogenic transfer or a series of gas expansions (2018, emails from Ellen R. M. Druffel and Ann P. McNichol to the authors; unreferenced, see "Acknowledgements") between V_1 and a reference flask of known volume (V_3) through a corridor (V_2). Therefore, we performed numerical simulations and error propagation of these two methods to determine whether the cold-finger volume uncertainties could be minimized through proper experimental design. Since the ultimate purpose of these tests is to minimize manometric uncertainty for ^{14}C-based studies, we then performed simple calculations to determine the ranges of moles of CO_2 that can be measured at the highest precision for different cold-finger volumes. Finally, we demonstrate the effects of these uncertainties on ^{14}C applications, such as simple conservative mixing calculations.

METHODS

It is well known that precise temperature control will improve determinations of V_1. However, three other common but often overlooked errors can arise.

First, the volumes in Figure 1 can change upon the actuating valves—most significantly, for example, when using high-vacuum glass valves seated with compressible o-rings. This error can be reduced by carefully defining the volumes with reproducible valve stem positioning, or virtually eliminated by instead using lightly-greased tapered glass stopcocks (e.g., Chemglass Cat. No. CG-473) or similarly flat-seated metal valves. Henceforth, our analyses assume manometric systems with tapered glass stopcocks that render this error negligible.

Second, the CDG sensing element is a capacitor with one plate that deflects when pressurized, effectively changing the volume of the cold-finger. Therefore, if warranted by measurement

https://doi.org/10.1017/RDC.2019.43 Published online by Cambridge University Press

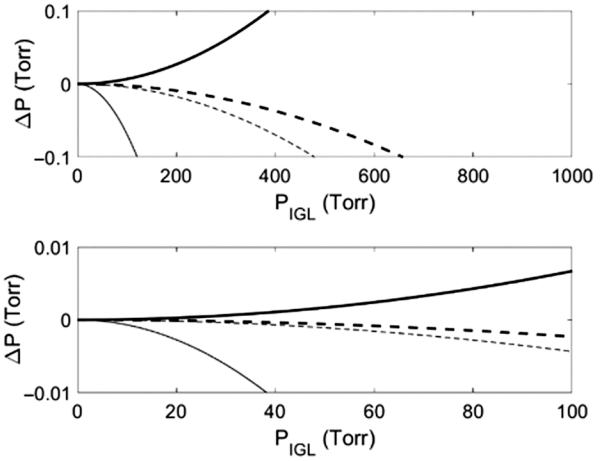

Figure 2 Deviations in calculated pressures from ideality ($\Delta P = P_{VE} - P_{IGL}$) of four gases (He = bold solid line, N_2 = bold dashed line, dry air = thin dashed line, CO_2 = thin solid line) over a range of pressures commonly measured on commercially available capacitance diaphragm gauges with measurable increments of (a) 0.1 Torr on a 999.9 Torr full-scale CDG and (b) 0.01 Torr on a 99.99 Torr full-scale CDG. Pressures were calculated for $V_1 = 15$ cm^3, $T = 298.15$ K, and B(T)'s of 12.44 cm^3 mol^{-1}, –4.3 cm^3 mol^{-1}, −127 cm^3 mol^{-1} and −8.0885 cm^3 mol^{-1} for He, N_2, CO_2, and dry air, respectively (Supplementary Materials, Figure S-1).

uncertainties, the most general determination should quantify V_1 at the CDG equilibrium position (i.e., $V_1 = V_{1,o}$ at $P = 0$ Torr) and parameterize the additional pressure-dependent volumes created when the diaphragm is deflected ($V_1 = V_{1,o} + \Delta V_1(P)$; Supplementary Materials).

Third, although the ideal gas law ("IGL," $PV = nRT$) is commonly used to determine V_1, measurable errors can arise if deviations from ideality exceed the increment of the pressure gauge (Figure 2; Supplementary Materials). More accurate results can be obtained with the truncated virial equation (VE), which is widely used for its accuracy and simplicity (Poling et al. 2001). It can be expressed as $PV = nRTZ$, where the compressibility factor (Z) is a series expansion in pressure or molar volume often truncated at the second term (e.g., $Z \approx 1 + BP/RT$), and the second virial coefficient (B) is a characteristic property of each gas at a given T. For example, pressures of the four gases commonly used to determine V_1 (He, N_2, CO_2, and dry air) deviate from those predicted with the ideal gas law by an amount exceeding the 0.1 Torr increment of a 999.9 Torr full-scale CDG at $P > \sim 600$ Torr in a 15 cm^3 cold-finger at 298.15 K (Figure 2a; Supplementary Materials). In contrast, only CO_2 deviates more than the 0.01 Torr increment of a 99.99 Torr full-scale CDG (Figure 2b). Accordingly, we used the virial equation in all simulated V_1 determinations but recommend the ideal gas law for error propagation and manometry at pressures where deviations are negligible (Figure 2).

Serial Gas Expansion Method

In this method, equilibrium pressures (P_1, P_{12}, P_{123}) and temperatures (T_1, T_{12}, T_{123}) are measured during a series of gas expansions from the cold-finger (V_1) into successively

https://doi.org/10.1017/RDC.2019.43 Published online by Cambridge University Press

larger volumes ($V_{12} = V_1 + V_2$, then $V_{123} = V_1 + V_2 + V_3$). The largest volume ($V_{123}$) includes a clean, dry reference flask (V_3) whose volume was previously determined gravimetrically with pure water (Figure 1). First, the system (V_1, V_2, and V_3) is thoroughly heated and evacuated ($P \leq 10$ mTorr) to remove all gases and residual water. After cooling to ambient temperature, valves B, C, and D are closed, the CDG is zeroed, and the cold-finger (V_1) is filled with dry gas via stopcock A (additional vent not shown). The equilibrium pressures and temperatures are measured after closing valve A (P_1, T_1, for V_1), again after expanding this gas into the corridor via valve B (P_{12}, T_{12}, for V_{12}), and lastly after expanding into the reference flask via valve D (P_{123}, T_{123}, for V_{123}). In the absence of leaks (real or virtual), surface attachment, or other artifacts, the number of moles of gas (n) remains constant during each expansion and the cold-finger volume (V_1) can be calculated via the truncated virial equation (Supplementary Materials). If $T_1 \approx T_{12} \approx T_{123}$ and changes in volume due to diaphragm deflections are negligible, then V_1 is readily calculated via Eq. (1), where $Z_1 = 1$ when the ideal gas law applies, or $Z_1 = 1 + BP(RT_1)^{-1}$ when it does not (B is a function of T_1); otherwise, it should be calculated via Eq. (S-7) (Supplementary Materials).

$$V_1 = \frac{1}{P_1}\left(\frac{1}{P_{123}} - \frac{1}{P_{12}}\right)^{-1} V_3 Z_1 \tag{1}$$

Cryogenic Transfer Method

Cryogenic transfer refers to the direct transfer of a condensable gas from the reference flask (V_3) to the cold-finger (V_1) using a cryogenic bath (Figure 1). This process eliminates measurements involving the corridor (P_{12}, T_{12}) with the potential for reducing uncertainty when calculating V_1. CO_2 is convenient for this method because it can be readily produced, dried, and condensed in a liquid nitrogen bath. However, CO_2 deviates significantly from ideality at most pressures of interest (Figure 2) and requires a "real" equation of state for greatest accuracy.

First, the system (V_1, V_2, and V_3) is heated and evacuated ($P \leq 10$ mTorr) to remove all gases and residual water. After cooling to ambient temperature, valve C is closed, the pressure gauge is zeroed, and the system is filled with dry, condensable gas via valve A. Next, after closing valve A and thermally equilibrating, the pressure and temperature are measured (P_3, T_3, for V_3), stopcock D is closed, and the gas in V_1 and V_2 is evacuated. Finally, the gas in the reference flask (V_3) is cryogenically transferred into the cold-finger, A and B are closed, the cold-finger is warmed, and the pressure and temperature are measured (P_1, T_1, for V_1). Assuming complete transfer, the absence of leaks (real or virtual), negligible surface attachment, etc., then the number of moles of gas (n) remains constant. If $T_1 \approx T_3$ and changes in volume due to CDG diaphragm deflection are negligible, then V_1 is readily calculated via Eq. (2); otherwise, it should be calculated via Eq. (S-21) (Supplementary Materials).

$$V_1 = \frac{P_3 Z_1}{P_1 Z_3} V_3 \tag{2}$$

Uncertainty Estimations

The uncertainties of measurements used in Eq. (1) or (2) propagate non-linearly to the total uncertainty of V_1. This suggests the relative uncertainty on V_1 can be minimized with an appropriate gas, optimal initial pressure, and/or optimal reference flask volume (V_3).

https://doi.org/10.1017/RDC.2019.43 Published online by Cambridge University Press

The influence of a gas choice on the uncertainty is easily reduced by choosing one with a compressibility factor that is least sensitive to pressure and temperature over the range of observed values (Figure 2, Figure S-1, and Supplementary Materials). The influences of V_3 and initial pressures are not as easily found. Therefore, we searched for optimal V_3's and initial pressures with numerical simulations using the virial equation and normally-distributed random noise added to each simulated measurement (MATLAB code available in Supplementary Materials). We also searched for optimum conditions analytically by propagating uncertainties as single standard deviations (σ_i) with Taylor series approximations of the ideal gas law (Bevington and Robinson 2002).

Simulated pressure measurements were based on two low-cost, commercially available CDGs commonly used for manometry in ^{14}C sample preparation laboratories: MKS Instruments' Baratron 626C13TAD (0.0–999.9 Torr range, 0.1 Torr increment) and Baratron 626C12TAD (0.00–99.99 Torr range, 0.01 Torr increment). Both have reported uncertainties equal to their pressure increments or 0.15% of their readings, whichever is greater. Although the actual uncertainty of a population of CDG measurements is not strictly given by this specification, the relative uncertainties of pressure measurements can be reasonably approximated by a piecewise continuous function with a cusp at $P_{cusp} \equiv increment/0.0015$ (2018, email from Dick Jacobs to the authors; unreferenced, see "Acknowledgements"). Therefore, we coded the relative uncertainty of pressure measurements according to Eq. (3).

$$\frac{\sigma_P}{P} = \begin{cases} 0.0015, P \geq P_{cusp} \\ \frac{P_{increment}}{P}, P < P_{cusp} \end{cases} \tag{3}$$

Reference flask volumes (V_3) were assumed to have been measured gravimetrically with pure water. The uncertainty in water mass was based on a typical laboratory balance (Metler Toledo XS304, $\sigma_m = 0.1$g) and assumed constant over the range of simulated V_3's. Relative uncertainties in water density due to uncertainty in T measurements were assumed negligible compared to relative uncertainties of mass. Thus, relative uncertainties of V_3 were coded as $\frac{\sigma_{V_3}}{V_3} = \frac{\sigma_{m_3}}{m_3}$ for $\rho_{water} = 0.9970470$ g cm^{-3} at T = 298.15 K (Rumble 2018).

Serial gas expansions were simulated in MATLAB over a range of cold-finger and corridor volumes typically encountered in sample preparation laboratories for ^{14}C analyses. These simulations were based on expansions of dry air because it exhibits small deviations from ideality (nearly the same as N_2; Figure 2) and is conveniently available to all laboratories equipped with drying tubes. First, a matrix of exact values of V_1 (1–31 cm^3; 1 cm^3 increment), V_2 (0–49 cm^3; 1 cm^3 increment), and V_3 (0.1–500.1 cm^3; 0.5 cm^3 increment) were prescribed for a total of $31 \times 50 \times 1001 = 1{,}551{,}550$ sets of virtual manometric systems with reference flasks. These cold-fingers volumes (V_1) were chosen because they fall within a range routinely used to measure sample masses with 999.9 Torr full-scale CDG's in the range required for graphite sputter ion source AMS (10 to 1000 μg C as CO_2). Likewise, the simulated corridor volumes chosen were also routinely found on sample prep lines. Finally, the range of simulated reference flask volumes were chosen based on the minimum and maximum volumes that can be quantified gravimetrically on a typical laboratory balance. In addition, preliminary uncertainty calculations suggested that larger reference flasks are neither practical nor necessary for achieving the best precision measurements of V_1. For each set of volumes, exact values of P_{12} and P_{123} were calculated from a range of starting pressures (P_1) at a typical laboratory temperature ($T_1 = 298.15$ K) using the virial equation of state. We then simulated 1000 replicate determinations of V_1 for each set by adding normally distributed random noise to

https://doi.org/10.1017/RDC.2019.43 Published online by Cambridge University Press

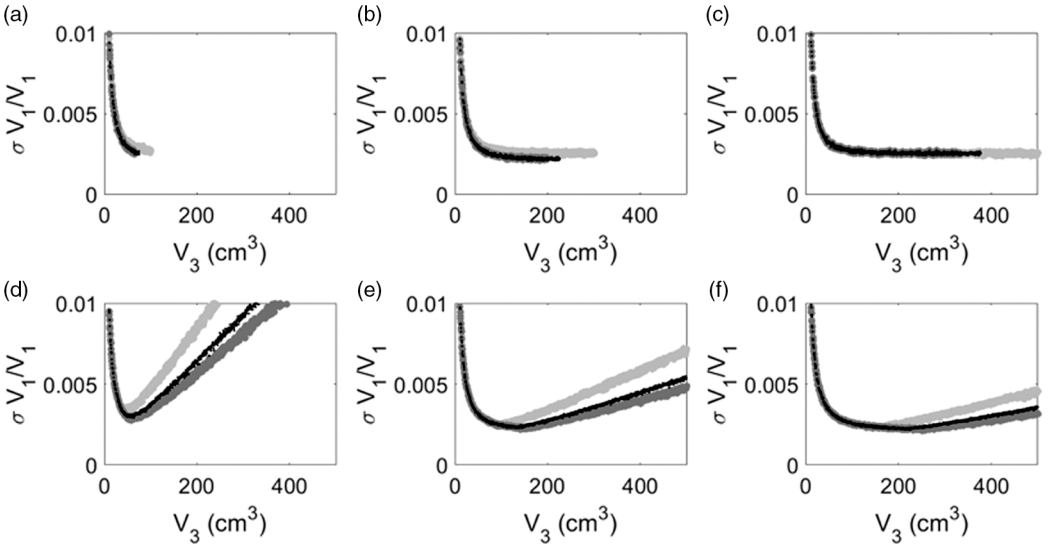

Figure 3 Examples of relative uncertainties on V_1 from cryogenic transfers (top row) and serial gas expansions (bottom row) vs. V_3 for cold-finger volumes (V_1) equal to 5 cm^3 (a and d), 15 cm^3 (b and e), and 25 cm^3 (c and f), assuming initial pressures of 50.0 Torr (light gray points), 66.7 Torr (black points), or 76.0 Torr (dark gray). T = 298.15K, B(T) = −127 cm^3 mol^{-1} for CO_2 and −8.0885 cm^3 mol^{-1} for dry air (Supplementary Materials, Figure S-1), and V_2 = 0 cm^3. Cryogenic transfers and serial gas expansions were simulated with 999.9 Torr and 99.99 Torr full-scale CDGs, respectively. Cryogenic transfer results are shown for V_3's with measurable final pressures (≤ 999.9 Torr), and therefore do not necessarily extend over the full range of V_3.

each value of P_1, P_{12}, P_{123}, and V_3. The average V_1 and standard deviation (σ_{V_1}) for each set of volumes were calculated, along with covariances between pressures and volumes. Finally, we identified the optimum reference flask volume (e.g., compression ratio = V_3/ V_1) that yielded the lowest relative uncertainties for each V_1 (i.e., $\frac{\sigma_{V_1}}{V_1}$). The mean values of simulated V_1's were equal to the prescribed values within uncertainty and had normally distributed standard deviations (Figure S-3; Supplementary Materials). This indicated that the uncertainties were symmetric and could be treated as single standard deviations during subsequent manometric analyses.

Numerical simulations of cryogenic transfers were similar to those of serial gas expansions, except that compression during transfer from a larger V_3 to a smaller V_1 dictated a smaller range of initial pressures and V_3's (Figure 3, top row) to prevent the final pressure from exceeding the range of the gauge. Correspondingly, these simulations used the "larger" 999.9 Torr full-scale CDG.

RESULTS AND DISCUSSION

The relative uncertainties on all V_1's determined by cryogenic transfer of CO_2 decreased asymptotically to ~0.0020 with increasing reference flask volumes (Figure 3, top row). If $V_3 > \sim 100$ cm^3, $V_1 > \sim 7$ cm^3 (i.e., 100 cm^3 × (66.7 Torr / 1000 Torr)), and the initial pressure was larger than P_{cusp} (66.7 Torr on the 999.9 Torr full-scale CDG), then the relative uncertainty was independent of reference flask volume and initial pressure. This insensitivity is reasonable because, in this range, all pressure measurements exhibit constant relative uncertainties (Eq. (3)), CO_2 exhibits small deviations from ideality (Z_{CO2} = 0.9932 at 298.15 K and 1000 Torr), and the

https://doi.org/10.1017/RDC.2019.43 Published online by Cambridge University Press

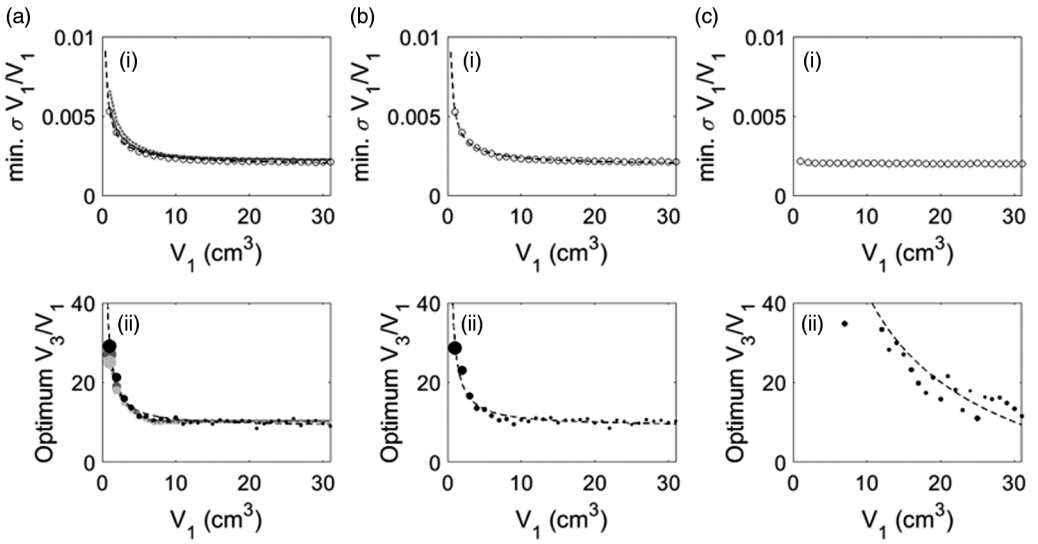

Figure 4 Numerically simulated minimum relative uncertainties of V_1 (Top row, circles) and optimum compression ratios (bottom row, black circles) as a function of V_1 measured under three different scenarios: serial gas expansions with the 99.99 Torr full-scale CDG and initial pressure = 76 Torr (a.i and a.ii), serial gas expansions with the 999.9 Torr full-scale CDG and initial pressure = 760 Torr (b.i and b.ii), cryogenic transfer with the 999.9 Torr full-scale CDG and initial pressure = 66.7 Torr (c.i and c.ii). All simulations are shown with least-squares fits to empirical power functions (black dashed lines; see text). The circle sizes in the bottom row correspond to the magnitude of the minimum σ_{V1}/V_1 from panels in the top row. Gray lines and dots in (a.i) and (a.ii) are results derived analytically by uncertainty propagation with Taylor series approximations for the case where $V_2 = 0$ cm^3 (dark gray) and $V_2 = 5$ cm^3 (light gray).

relative uncertainty of V_3 is independent of pressure measurements (Eq. S-27; Supplementary Materials). In addition, the minimum relative uncertainties on V_1 were independent of the volume of V_1 (Figure 4c.i). The corresponding optimum compression ratios were not clearly identifiable (Figure 4c.ii), consistent with the results shown in Figure 3 (top row). However, the optimum compression ratio (V_3/V_1) must be less than ~15 under the conditions studied here to prevent CO_2 with a minimum initial pressure = P_{cusp} (66.7 Torr) from exceeding the CGD's maximum measurable pressure (999.9 Torr) after transfer to V_1.

In contrast, the relative uncertainties for all V_1 determinations by serial gas expansion exhibited clearly identifiable minima with respect to reference flask volumes, regardless of initial pressure (Figure 3, bottom row). Larger cold-fingers exhibited slightly lower minima that were also broader and associated with larger "optimal" reference flask volumes. Combined, these results suggest that the highest precision measurements of V_1 can be achieved on larger cold-fingers without the need for a precisely optimized reference flask volume. However, the relative uncertainties were asymmetric functions of V_3 that were most sensitive to reference flasks with volumes smaller than the optimum. For example, 5 cm^3, 15 cm^3, and 25 cm^3 cold-fingers had simulated minimum achievable relative uncertainties of 0.0028, 0.0022, and 0.0021 when measured with optimally-sized reference flasks (58 cm^3, 145 cm^3, and 252 cm^3, respectively), and a starting pressure of 76 Torr (Figure 3d, e, f). If, instead, they were all measured with the same non-optimally-sized 30 cm^3 reference flask, then the minimum achievable relative uncertainties on these cold-finger volumes would increase by 46%, 95%, and 129% to 0.0041, 0.0043, and 0.0048, respectively. Therefore, we recommend choosing reference flasks with

https://doi.org/10.1017/RDC.2019.43 Published online by Cambridge University Press

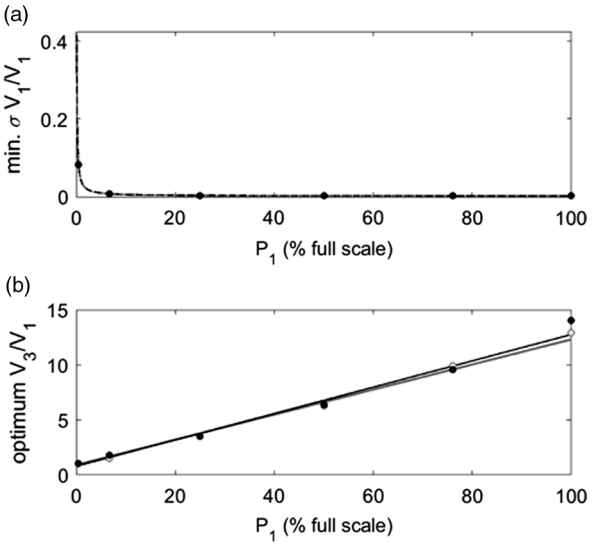

Figure 5 (a) Minimum achievable relative uncertainties and (b) associated optimum compression ratios (V_3/V_1) as a function of initial pressure (P_1, expressed as % full-scale reading) for serial gas expansions of dry air at 298.15 K, with $B(T) = -8.0885$ cm^3 mol^{-1} (Supplementary Materials, Figure S-1), and $V_1 = 15$ cm^3. Results were calculated for the 99.99 Torr (black dots) and 999.9 Torr (gray dots) full-scale CDG's. Least squares fits to empirical power and linear functions for the 99.99 Torr full-scale CDG (black lines) and the 999.9 Torr full-scale CDG (gray lines).

volumes that are equal to, or slightly larger than, the optimum volume for a given initial estimate of each cold-finger's volume.

The minimum relative uncertainties of V_1 determined by serial gas expansion (e.g., the minima in Figure 3, bottom row) decreased asymptotically with increasing starting pressure ($\frac{\sigma_{V_1}}{V_1} = (0.0398 \pm 0.0001)P_1{}^{(-1.02 \pm 0.01)} + (0.00172 \pm 0.00005)$, $r^2 = 1$; Figure 5). This relationship was identical for both CDG's when expressing pressure as a percentage of full-scale. For example, relative uncertainties on a 15 cm^3 cold-finger were largely independent of starting pressures greater than ~50% full-scale, reaching a minimum of ~0.0020 at 100% full-scale (Figure 5a). Since higher initial pressures will not significantly improve relative uncertainties, it is both convenient and effective to determine V_1 with dry air at an initial pressure of ~760 Torr (ambient pressure) for the 999.9 Torr full-scale CDG using an optimally sized reference flask ($V_3/V_1 \approx 10$; Figure 4b). We likewise advocate determining V_1 with an initial pressure of ~76% full-scale on the 99.99 Torr gauge to minimize the risk of errors associated with measurements near the CDG's upper limit.

Unlike the cryogenic transfer method, the minimum achievable relative uncertainties of V_1 determined by serial gas expansion also depended on V_1. For example, the minimum $\frac{\sigma_{V_1}}{V_1}$ and optimum compression ratios decreased asymptotically to 0.0021 and ~10, respectively, with increasing V_1 up to 30 cm^3 for initial pressures equal to 76% of the full-scale reading and $V_2 = 0$ cm^3 (Figure 4a's and b's). This limit on the relative uncertainty was nearly

https://doi.org/10.1017/RDC.2019.43 Published online by Cambridge University Press

achievable for all V_1 exceeding ~12 cm^3 on both CDG's. Nevertheless, a cold-finger equipped with the 99.99 Torr full-scale CDG precludes the need for the virial equation in V_1 determinations ($Z = 1$ in Eq. (1); Figure 2) and potentially has greater sensitivity and lower detection limits during routine manometric measurements.

Finally, the presence of a corridor ($V_2 > 0$ cm^3) necessarily increases the minimum achievable relative uncertainty by virtue of an additional measurement (e.g., Eq. S-18). Therefore, if so required, the absolute minimum achievable relative uncertainty could be obtained by permanently welding an optimally-sized reference flask directly to each cold-finger (i.e., $V_2 = 0$ cm^3), to permit redeterminations of V_1 following repairs or off-site CDG calibrations. However, the additional relative uncertainty of V_1 due to the presence of a small corridor is negligible compared to a system without a corridor (Figure 4a's). This is supported by the partial derivatives of Eq. (1) where a small corridor and large compression ratio minimizes the weight of uncertainty from P_{12} on V_1 (Supplementary Materials, Eq. S-15). Therefore, we recommend using a small corridor in a manometric system, if possible, for its convenience in replacing, repairing, and testing various reference flasks and cold-fingers.

Collectively, optimized serial gas expansions with dry air are an effective, simple, low-cost, and safe method for determining cold-finger volumes. The method only requires a properly sized flask, a desiccant, and basic knowledge of vacuum manipulations and associated hazards (Shriver and Drezdzon 1986). An analyst can use empirical fits to our simulated data (Figure 4a's and b's), such that $V_{3,optimum} = (V_3/V_1)_{opt} \times V_{1,estimated}$) and initial estimates of cold-finger volumes (based on design parameters) to determine the optimal reference flask volumes and predict the ensuing minimum relative uncertainty on V_1 when using these, or comparable, CDGs.

$$\left(\frac{V_3}{V_1}\right)_{opt.} = 20.8V_1^{-1.0} + 8.95 \tag{4}$$

$$\left(\frac{\sigma_{V_1}}{V_1}\right)_{min.} = 0.003478V_1^{-0.8094} + 0.001844 \tag{5}$$

For systems that use a different CDG, an analyst may input the associated uncertainty function into our MATLAB code (Supplementary Materials) to estimate the minimum relative uncertainties on their cold-fingers and the optimum sizes of the reference flasks required to achieve them.

The ultimate purpose of optimizing V_1 measurements is to improve the precision of P-V-T measurements of moles of carbon (n). When the ideal gas law applies (Figure 2), the relative uncertainty of gas mole measurements ($\frac{\sigma_n}{n}$) can be calculated with Eq. (6).

$$\frac{\sigma_n}{n} = \sqrt{\left(\frac{\sigma_P}{P}\right)^2 + \left(\frac{\sigma_{V_1}}{V_1}\right)^2 + \left(\frac{\sigma_T}{T}\right)^2} \tag{6}$$

Assuming the volume of a cold-finger fitted with either of these CDGs is measured with an optimally sized reference flask and the temperature is stable, then variations in the relative uncertainty as a function of n will depend on the relative uncertainty of pressure (Eq. (3)) for any fixed V_1. Additionally, the minimum achievable relative uncertainty of n will be relatively constant for all V_1 exceeding ~12 cm^3 on both CDG's (~0.0026 to ~0.0027, Figure 6) because

https://doi.org/10.1017/RDC.2019.43 Published online by Cambridge University Press

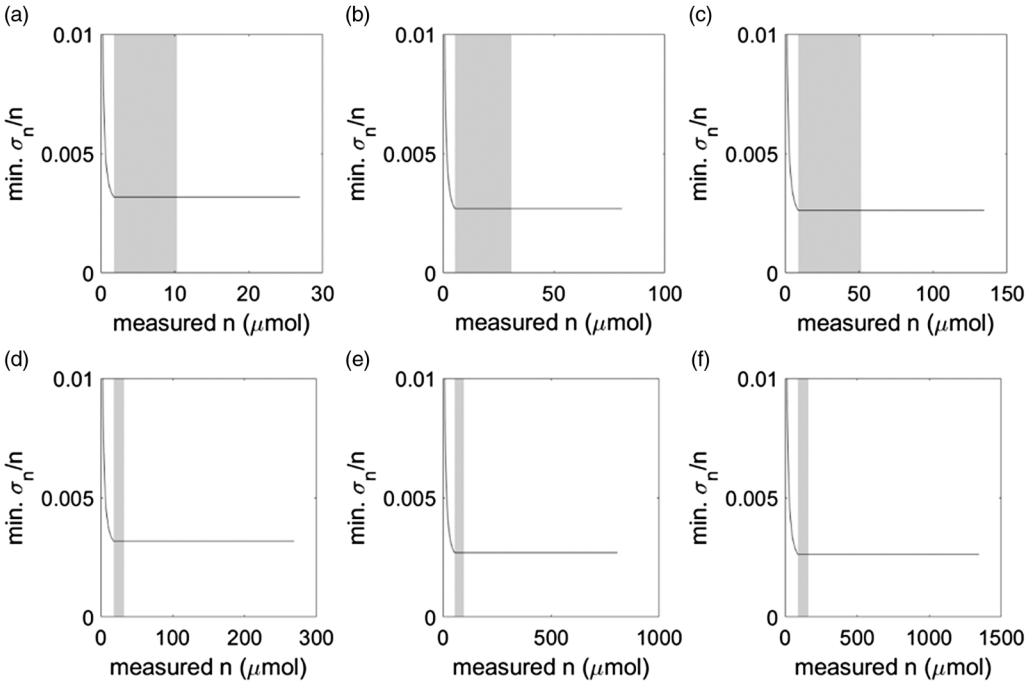

Figure 6 Minimum achievable relative uncertainty of moles of CO_2 (σ_n/n) as a function of moles of CO_2 (n) from simulated measurements with the 99.99 Torr full-scale (top row) and 999.9 Torr full-scale (bottom row) CDGs and cold-finger volumes (V_1) equal to 5 cm^3 (a and d), 15 cm^3 (b and e), and 25 cm^3 (c and f). The relative uncertainties were calculated with the ideal gas law, assuming each V_1 was calibrated optimally, T = 298.15 K, and $\sigma_T = \pm 0.1$ K. The relative uncertainties (solid lines) were calculated for n's with measurable final pressures ($\leq$ 100% full-scale of CDG's), and therefore do not extend across the n axis. Gray shaded areas span the ranges of n that can be measured with the lowest relative uncertainties and minimal errors using the ideal gas law.

$\frac{\sigma_{V_1}}{V_1}$ varies little for all V_1 in this range (Figure 4a.i). Therefore, the optimum choice of V_1 for any application depends on the sample sizes (moles of CO_2) that will be routinely measured (Figure 6). Samples that generate pressures below P_{cusp} will significantly increase the relative uncertainty of P, while pressures exceeding the applicability of the ideal gas law will impart errors unless a more realistic equation of state is used. Accordingly, the optimum V_1 for a given application should be chosen so that, when the routine number of moles of CO_2 is isolated in the cold-finger, the pressure at room temperature should be 6.67 to 38.26 Torr for 99.99 Torr full-scale CDG, and 66.7 to 120.9 Torr for 999.9 Torr full-scale CDG. For example, samples ranging from ~1.8 to ~10.3 µmol are best measured with a 99.99 Torr full-scale CDG and a 5 cm^3 cold-finger, from ~5.4 to ~30.9 µmol with a 15 cm^3 cold-finger, and from ~9.0 to ~51.4 µmol a 25 cm^3 cold-finger (Figure 6, top row, gray shaded areas). Likewise, samples ranging from ~17.9 to ~32.5 µmol are best measured with a 999.9 Torr full-scale CDG and a 5 cm^3 cold-finger, from ~53.8 to ~97.5 µmol with a 15 cm^3 cold-finger, and from ~89.7 to ~162.6 µmol a 25 cm^3 cold-finger (Figure 6, bottom row, gray shaded areas). Based on these results, an apparatus that routinely generates ~1 mg C for routine ^{14}C analyses can be measured most precisely with the 999.9 Torr CDG fixed to an optimally measured ~15 cm^3 cold-finger.

Hence, optimized V_1 measurements are most important for direct measurements of the yields of routine radiocarbon standards, blanks, and samples (Schuur et al. 2016), as well as measurements of the absolute number of ^{14}C atoms in special applications (Roberts and

https://doi.org/10.1017/RDC.2019.43 Published online by Cambridge University Press

Southon 2007). For example, optimization reduces the relative uncertainty of manometric experimental yields ($\left(\frac{\sigma_n}{n}\right)_{optimized} = 0.0026$ to 0.0027) to nearly those of gravimetric theoretical yields of 1 mg C from IAEA sucrose (~0.0042) or Oxalic acid (~0.0019) using a typical balance (± 0.01 mg). The influence of manometric uncertainty on ^{14}C analyses depends on the property that is to be calculated. For example, the ^{14}C signature of one component in a mixture ($\Delta^{14}C_1$) can be calculated from the moles and $\Delta^{14}C$ values of the mixture (n_{mix}, $\Delta^{14}C_{mix}$) and of the other component (n_2, $\Delta^{14}C_2$), such as a blank (Eq. (7)).

$$\Delta^{14}C_1 = \frac{\Delta^{14}C_{mix}n_{mix} - \Delta^{14}C_2 n_2}{n_{mix} - n_2} \tag{7}$$

Hence the uncertainty of the $\Delta^{14}C_1$ ($\sigma_{\Delta^{14}C_1}$) can be calculated as Eq. (8).

$$\sigma_{\Delta^{14}C_1} = \sqrt{\left(\frac{\partial\Delta^{14}C_1}{\partial\Delta^{14}C_{mix}}\right)^2\sigma^2_{\Delta^{14}C_{mix}} + \left(\frac{\partial\Delta^{14}C_1}{\partial\Delta^{14}C_2}\right)^2\sigma^2_{\Delta^{14}C_2} + \left(\frac{\partial\Delta^{14}C_1}{\partial n_{mix}}\right)^2\sigma^2_{n_{mix}} + \left(\frac{\partial\Delta^{14}C_1}{\partial n_2}\right)^2\sigma^2_{n_2}} \tag{8}$$

The partial derivatives in Eq. (8) represent how sensitive the uncertainty on the calculated value ($\sigma_{\Delta^{14}C_1}$) is to each of the measured quantities, and are given by Eq. (9) to (12).

$$\left(\frac{\partial\Delta^{14}C_1}{\partial\Delta^{14}C_{mix}}\right) = \frac{n_{mix}}{n_{mix} - n_2} \tag{9}$$

$$\left(\frac{\partial\Delta^{14}C_1}{\partial\Delta^{14}C_2}\right) = \frac{-n_2}{n_{mix} - n_2} \tag{10}$$

$$\frac{\partial\Delta^{14}C_1}{\partial n_{mix}} = \left(\frac{\partial\Delta^{14}C_1}{\partial\Delta^{14}C_2}\right)\gamma \tag{11}$$

$$\frac{\partial\Delta^{14}C_1}{\partial n_2} = \left(\frac{\partial\Delta^{14}C_1}{\partial\Delta^{14}C_{mix}}\right)\gamma \tag{12}$$

where $\gamma = \left(\Delta^{14}C_{mix} - \Delta^{14}C_2\right)/(n_{mix} - n_2)$. Based on these partial derivatives, the calculation will be most sensitive to manometric uncertainty when the mixture and the known component have a similar number of moles but significantly different $\Delta^{14}C$ values (i.e., large γ). For example, 5.4 µmol of CO_2 measured in a 15 cm^3 cold-finger with the 99.99 Torr full-scale CDG would have a minimum relative uncertainty of ~0.0027 (Figure 6) and a corresponding uncertainty of $\sigma_n \approx 0.01$ µmol. If $\Delta^{14}C$ values are routinely measured to better than ca. ± 5 ‰, then γ must be larger than approximately 500 in order for manometric uncertainty to dominate the calculation of $\Delta^{14}C_1$. However, if n was measured with a sub-optimal manometric system, such that $\frac{\sigma_{V_1}}{V_1} = 0.0043$ and $\frac{\sigma_n}{n} = 0.0046$, then γ would only have to be greater than ca. 300, making the calculation significantly more sensitive to manometric uncertainty. Therefore, this calculation would be less vulnerable to manometric uncertainties over a broader range of sample compositions if V_1 were to be measured optimally. Similar sensitivity studies should be performed for all ^{14}C calculations to optimize experimental designs.

CONCLUSIONS

Numerical simulations and analytical uncertainty propagation demonstrate that relative uncertainties of cold-finger volumes can be minimized through determinations with optimal

https://doi.org/10.1017/RDC.2019.43 Published online by Cambridge University Press

reference flask volumes and initial pressures. The minimum achievable relative uncertainty of V_1 by either of the two tested methods over the range of parameters studied here is ~0.002. Optimized serial gas expansions are favored over cryogenic transfers for determining cold-finger volumes due to their convenience, despite marginally larger minimum achievable relative uncertainties (by ~0.0001). Since the relative uncertainty of cold-finger volumes is insensitive to initial pressures greater than ~50% full-scale, we advocate using serial gas expansions with dry air at ~76% full-scale and choosing an optimum reference flask volume via Eq. (4). Furthermore, based on Eq. (5), the lowest relative uncertainty of cold-finger volume measurements (between 0.0021 and 0.0023) can be achieved using the smallest possible corridor (V_2) with a cold-finger greater than or equal to ~12 cm^3. Under these conditions, the minimum achievable relative uncertainties correspond to absolute volume uncertainties that are slightly larger than the additional volumes created by CDG diaphragm deflections during V_1 determinations. Therefore, the CDG deflection volumes may be safely ignored without significantly reducing accuracy.

If the manometric system is set up as recommended using comparable CDG's, then the relative uncertainty of mole measurements will be minimized to between ~0.0026 and ~0.0027 (Figure 6). Likewise, ^{14}C-based calculations will be less vulnerable to manometric uncertainties over a broader range of sample compositions if V_1 is measured optimally. If higher precision is needed, then the manometric system could employ a higher precision pressure gauge and/or be housed in a temperature-controlled oven (Zhao et al. 1997). However, if the higher precision gauge is a capacitance manometer, then determinations of V_1 and subsequent manometric measurements must include corrections for volume changes due to diaphragm deflections, which can be parameterized as $V = V_{1,o} + \Delta V(P)$, where $V_{1,o}$ is the volume of the cold-finger at 0 Torr and $\Delta V(P) \approx (\Delta V_{max}/P_{max}) \times P$ (see derivations in Supplementary Materials). Ultimately, all of these efforts to optimize cold-finger volume measurements are practical, low-cost approaches that could improve the precision of manometric measurements and our ability to answer scientific questions.

ACKNOWLEDGMENTS

This work was supported under NSF grant OCE-1536597 and a Minghua Zhang Early Career Faculty Innovation Award to S. R. Beaupré. We thank Dick Jacobs (MKS Instruments, Inc.), Ellen R. M. Druffel (University of California, Irvine), and Ann P. McNichol (Woods Hole Oceanographic Institution) for intellectual support, and two anonymous reviewers for helpful comments. The authors declare no competing financial interests.

SUPPLEMENTARY MATERIAL

To view supplementary material for this article, please visit https://doi.org/10.1017/RDC.2019.43

REFERENCES

Beaupré SR, Druffel ERM, Griffin S. 2007. A low-blank photochemical extraction system for concentration and isotopic analyses of marine dissolved organic carbon. Limnology and Oceanography: Methods 5:174–184.

Beaupré SR, Mahmoudi N, Pearson A. 2016. IsoCaRB: a novel bioreactor system to characterize the lability and natural carbon isotopic (^{14}C, ^{13}C) signatures of microbially respired organic matter. Limnology and Oceanography: Methods 14(10):668–681.

Bevington PR, Robinson DK. 2002. Data reduction and error analysis for the physical sciences. New York, NY: The McGraw-Hill Companies, Inc.

Gospodinova K, McNichol AP, Gagnon A, Shah Walter SR. 2016. Rapid extraction of dissolved inorganic carbon from seawater and groundwater samples for radiocarbon dating. Limnology and Oceanography: Methods 14(1):24–30.

Hamme RC, Emerson SR. 2004. Measurement of dissolved neon by isotope dilution using a quadrupole mass spectrometer. Marine Chemistry 91:53–64.

Hyland RW, Shaffer RL. 1991. Recommended practices for the calibration and use of capacitance diaphragm gages as transfer standards. Journal of Vacuum Science & Technology A: Vacuum, Surfaces, and Films 9(6):2843–2863.

Leigh McCallister S, del Giorgio PA. 2008. Direct measurement of the $d^{13}C$ signature of carbon respired by bacteria in lakes: linkages to potential carbon sources, ecosystem baseline metabolism, and CO_2 fluxes. Limnology and Oceanography 53(4):1204–1216.

Poling BE, Prausnitz JM, O'Connell JP. 2001. The properties of gases and liquids. New York, NY: The McGraw-Hill Companies, Inc.

Rees ED, Ross A. 1964. Optimal selection of flasks for the indirect method of manometry. Analytical Biochemistry 7:275–287.

Reimer PJ, Baillie MG, Bard E, Bayliss A, Beck JW, Bertrand CJ, Blackwell PG, Buck CE, Burr GS, Cutler KB. 2004. IntCal04 terrestrial radiocarbon age calibration, 0–26 cal kyr BP. Radiocarbon 46(3):1029–1058.

Reimer PJ, Baillie MG, Bard E, Bayliss A, Beck JW, Blackwell PG, Bronk RC, Buck CE, Burr GS, Edwards RL. 2009. IntCal09 and Marine09 radiocarbon age calibration curves, 0–50,000 years cal BP. Radiocarbon 51(4):1111–1150.

Reimer PJ, Bard E, Bayliss A, Beck JW, Blackwell PG, Ramsey CB, Buck CE, Cheng H, Edwards RL, Friedrich M. 2013. IntCal13 and Marine13 radiocarbon age calibration curves 0–50,000 years cal BP. Radiocarbon 55(4):1869–1887.

Roberts ML, Southon JR. 2007. A preliminary determination of the absolute $^{14}C/^{12}C$ ratio of OX-I. Radiocarbon 49(2):441–445.

Rumble JR Jr, editor. 2018. CRC Handbook of Chemistry and Physics. Boca Raton, FL: CRC Press/Taylor & Francis.

Schuur EAD, Druffel ERM, Trumbore SE, editors. 2016. Radiocarbon and climate change. Switzerland: Springer International Publishing Switzerland.

Shah Walter SR, Gagnon AR, Roberts ML, McNichol AP, Gaylord MCL, Klein E. 2015. Ultra-small graphitization reactors for ultra-microscale ^{14}C analysis at the National Ocean Sciences Accelerator Mass Spectrometry (NOSAMS) facility. Radiocarbon 57(1):109–122.

Shriver DF, Drezdzon MA. 1986. The manipulation of air-sensitive compounds. New York, NY: Wiley-Interscience.

Zhao CL, Tans PP, Thoning KW. 1997. A high precision manometric system for absolute calibrations of CO_2 in dry air. Journal of Geophysical Research: Atmospheres 102(D5):5885–5894.

https://doi.org/10.1017/RDC.2019.43 Published online by Cambridge University Press